JOURNAL OF VIROLOGY, Aug. 2009, p. 8173–8181 Vol. 83, No. 16
0022-538X/09/$08.00+0 doi:10.1128/JVI.00686-09

The Polycomb Group Protein Bmi1 Binds to the Herpes Simplex Virus 1 Latent Genome and Maintains Repressive Histone Marks during Latency[▽]

Dacia L. Kwiatkowski,[1] Hilary W. Thompson,[2] and David C. Bloom[1]*

Department of Molecular Genetics & Microbiology, University of Florida College of Medicine, Gainesville, Florida,[1] and Section of Biostatistics, School of Public Health, Louisiana State University Health Sciences Center, New Orleans, Louisiana[2]

Received 2 April 2009/Accepted 26 May 2009

The mechanism by which herpes simplex virus 1 (HSV-1) establishes latency in sensory neurons is largely unknown. Recent studies indicate that epigenetic modifications of the chromatin associated with the latent genome may play a key role in the transcriptional control of lytic genes during latency. In this study, we found both constitutive and facultative types of heterochromatin to be present on the latent HSV-1 genome. Deposition of the facultative marks trimethyl H3K27 and histone variant macroH2A varied at different sites on the genome, whereas the constitutive marker trimethyl H3K9 did not. In addition, we show that in the absence of the latency-associated transcript (LAT), the latent genome shows a dramatic increase in trimethyl H3K27, suggesting that expression of the LAT during latency may act to promote an appropriate heterochromatic state that represses lytic genes but is still poised for reactivation. Due to the presence of the mark trimethyl H3K27, we examined whether Polycomb group proteins, which methylate H3K27, were present on the HSV-1 genome during latency. Our data indicate that Bmi1, a member of the Polycomb repressive complex 1 (PRC1) maintenance complex, associates with specific sites in the genome, with the highest level of enrichment at the LAT enhancer. To our knowledge, these are the first data demonstrating that a virus can repress its gene transcription to enter latency by exploiting the mechanism of Polycomb-mediated repression.

After primary infection by herpes simplex virus 1 (HSV-1) in mucosal epithelia, the virus enters sensory neurons, where it can persist as a transcriptionally silent extrachromosomal episome (19). The only abundant transcription that occurs during latency is from a diploid gene in the repeat long segment of the virus that produces the latency-associated transcript (LAT), an 8.3- to 8.5-kb noncoding RNA (20, 21). The LAT is detectably expressed in only one-third of neurons that contain latent HSV genomes (9, 16). Following a reactivation stimulus, some of the latent genomes can exit this state to actively express lytic transcripts and produce new virus. The mechanism by which the genome establishes and maintains this latent state is currently unknown, although it is hypothesized that the reversible nature of the latent phase involves the constant interplay between cellular and viral factors that either keep the viral genome repressed or allow for reactivation.

Recent studies have shed light on epigenetic modifications to the HSV-1 genome during the establishment and maintenance of latency. As the genome enters the latent phase in the mouse, an accumulation of the histone mark dimethyl H3 lysine 9 (diMe H3K9), historically known as a transcriptionally repressed marker, is observed on lytic genes, while enrichment of the transcriptionally active histone mark dimethyl H3 lysine 4 (diMe H3K4) decreases (24). Furthermore, once the virus has established latency, the LAT region is enriched in the transcriptionally active marks, acetylated histone H3 lysines 9 and 14 and diMe H3K4 in mice and rabbits, respectively, compared to the lytic genes encoding ICP27 and ICP0 (8, 13, 14). These studies suggest that the virus can associate with cellular enzymes responsible for catalyzing histone posttranslational modifications (PTMs) and that these PTMs on HSV-1 genes can reflect their transcriptional status. The studies mentioned above looked only at euchromatic (transcriptionally permissive) marks on the genome, with the exception of the study by Wang et al. (24). However, in the study by Vakoc et al., the examined diMe H3K9 PTM has been shown to be present in both types of chromatin, euchromatin (transcriptionally permissive) and heterochromatin (transcriptionally nonpermissive) (23). In the present study, we sought to determine whether there was an association between the HSV-1 lytic genes and heterochromatin during latency. Determining the composition of the heterochromatin would not only indicate the nature of repression of the HSV-1 lytic genes during latency but could also elucidate the cellular and viral factors that mediate this repression.

Heterochromatin can be divided into two categories, constitutive and facultative (22). Though both are transcriptionally silent, each has distinct characteristics. Briefly, constitutive heterochromatin exists in a tightly compact 30-nm structure and will remain in a repressed state after the PTMs have been established (e.g., on centromeres and telomeres). In facultative heterochromatin, the order of compaction can vary but it retains the functional ability to convert between heterochromatin and euchromatin (e.g., on the X inactive chromosome and HOX genes). Furthermore, both types of heterochromatin are deposited and maintained by different proteins, making each method of repression distinct. Because HSV-1 can reactivate in response to a stress stimulus, it seems likely that the repres-

* Corresponding author. Mailing address: Department of Molecular Genetics & Microbiology, Box 100266, University of Florida College of Medicine, Gainesville, FL 32610-0266. Phone: (352) 392-8520. Fax: (352) 392-3133. E-mail: dbloom@ufl.edu.

▽ Published ahead of print on 10 June 2009.

sion controlling latency is reversible. Therefore, we hypothesized that the latent HSV-1 genome is repressed, at least in part, by the deposition of facultative heterochromatin since its repression is reversible. To investigate what type of heterochromatin is present on the genome during latency, we performed chromatin immunoprecipitation (ChIP) assays on the dorsal root ganglia (DRG) of mice latently infected with HSV-1 strain 17*syn*+. We examined the presence of trimethyl H3K27 (triMe H3K27), a PTM representative of facultative heterochromatin, as well as the presence of histone variant macroH2A, which is enriched in facultative heterochromatin and can directly inhibit transcription (5). In addition, we examined the latent genome for the presence of a constitutive heterochromatin PTM, trimethyl H3K9 (triMe H3K9).

Finally, since HSV-1 recombinants lacking the LAT promoter have previously been shown to possess a leakier lytic transcription profile during latency (2), we examined the presence of facultative marks on the LAT promoter deletion virus, 17ΔPst. Here we demonstrate that in the absence of the LAT, both triMe H3K27 and macroH2A are dramatically increased. This indicates that the LAT plays an important role in directing the chromatinization of the HSV-1 genome during latency and may explain why LAT mutants exhibit a decreased ability to reactivate from latency.

MATERIALS AND METHODS

Viruses and cells. ChIP experiments were performed using ganglia from mice infected with either 17*syn*+ or 17ΔPst. Both viruses were from low-passage stocks; 17*syn*+ was obtained from J. Stevens and 17ΔPst was constructed, as previously described, with a 202-bp deletion that removes the LAT transcriptional start site (4). Viruses were amplified and titrated on rabbit skin cells using Eagle's minimal essential medium (Life Technologies) supplemented with 5% calf serum, 250 U of penicillin/ml, 250 μg of streptomycin/ml, and 292 μg of L-glutamine/ml (Life Technologies).

Mouse infections. Four- to six-week-old outbred ND4 Swiss mice (Harlan Sprague Dawley, Inc.) were anesthetized by isoflurane inhalation and pretreated with 0.05 ml of a 10% (wt/vol) sterile saline solution injected into each rear footpad. At 3 h posttreatment, mice were anesthetized by intramuscular injection of 0.020 ml of a cocktail consisting of acepromazine (2.5 to 3.75 mg/kg of body weight), xylazine (7.5 to 11.5 mg/kg), and ketamine (30 to 45 mg/kg). The rear footpads were lightly abraded with an emery board to remove the keratinized epithelia. A virus inoculum of 500 PFU/0.05 ml per mouse was then applied to the feet. The virus was allowed to adsorb for 30 to 45 min while the mice remained on their backs. Mice were sacrificed at >28 days postinfection, and care was taken to ensure that the ganglia were removed and processed as quickly as possible postmortem (3 to 5 min per mouse).

ChIP. ChIPs were performed as previously described (13). Briefly, DRG from three mice per ChIP were collected at a minimum of 28 days postinfection. Tissue was homogenized, and the chromatin was fixed using formaldehyde (final concentration of 1%) and washed as previously described. Immunoprecipitations were performed on sonicated samples overnight at 4°C while shaking. Anti-triMe H3K27 (Millipore 07-449), anti-macroH2A (Millipore 07-219), and anti-Bmi1 (Millipore 05-637) were used at a concentration of 5 μg per sample. Anti-triMe H3K9 (Millipore 07-442) was used at a concentration of 4 μg per sample. Antibody complexes were captured using salmon sperm DNA-protein A agarose beads and washed in accordance with Millipore's protocol. Samples were decrosslinked and digested with RNase A and proteinase K, and the DNA was purified (Qiagen). Unbound and bound fractions were analyzed by TaqMan real-time PCR in triplicate on a Step-One Plus thermocycler (Applied Biosystems). Samples were analyzed as a bound/(unbound + bound) ratio [B/(U+B)] to represent the bound/input ratio and then normalized to a cellular control B/(U+B). Significance of enrichment between different genes was determined using analysis of variance (ANOVA). All ChIPs were validated using cellular targets enriched and depleted in the protein of interest. Additionally, a negative control ChIP was performed using rabbit control immunoglobulin G (IgG; Abcam Ab46540) at a concentration of 2 μg per sample. Primer/probe sequences for validation of these ChIPs are as follows: midline fwd. primer (rGGTCAGC CGTTTAGACTGGAT), rev. primer (CGTGGGACACCTTCAGCTT), probe (CCCAAATCGGCTCATCG); upHoxa5 fwd. primer (AGCAGCAGGGCCAA TTCT), rev. primer (GCTGCCCAAGCCAGCTT), probe (CCCGCGATGCA CCC); adenine phosphoribosyltransferase (APRT) fwd. primer (CTCAAGAA ATCTAACCCCTGACTCA), rev. primer (GCGGGACAGGCTGAGA), probe (CCCCACACACACCTC); mouse centromere fwd. primer (TGGCGAGGAA AACTGAAAAAGGT), rev. primer (TTTTCTTGCCATATTCCACGTCCTA), probe (CAGTGGACATTTCTAAATTT); mouse HOTAIR fwd. primer (GAT CTGACCACGCACATCTATCTC), rev. primer (CCCCAGCTCAGCTGCTC), probe (CCGCACACGCACTCAG); and MyoD1 fwd. primer (GGCCTTCGAG ACGCTCAA), rev. primer (GCGCAGGATCTCCACCTT), probe (CAGCAA CCCGAACCAG).

Data analysis methods. Corrected B/(U+B) ratios normalized to APRT B/(U+B) for the various primers were analyzed within each immunoprecipitation using a nested design in the ANOVA (17). Differences between primers among the virus strains by their respective immunoprecipitations were evaluated by a similar nested ANOVA using two factors, immunoprecipitation antibody and primer, and the interaction of these factors. Comparisons of primer means in both analyses were conducted using alpha level correction with a simulation method (6).

RNA and DNA isolation. Latently infected mouse DRG were homogenized in guanidine thiocyanate (GTC) solution and processed as previously described for the RNA preparation (3). An aliquot of the homogenized tissue was removed for the DNA preparation (12). After high-speed centrifugation (30,000 rpm) for 12 to 16 h, the RNA pellet was dissolved in water and precipitated overnight. RNA was pelleted and resuspended in RNase-free water. cDNA was synthesized simultaneously in seven separate reactions using random decamers and then pooled to allow for detection of low-abundance transcripts. TaqMan real-time PCR was performed on the cDNA and DNA preparations and analyzed as RNA molecules per genome.

RESULTS

HSV-1 lytic genes are enriched in triMe H3K27. To investigate if the latent HSV-1 genome was enriched in triMe H3K27, a marker of facultative heterochromatin, we performed ChIP on DRG dissected from 17*syn*+ latently infected mice. Relative quantities determined by real-time TaqMan PCR were analyzed as B/(U+B) and normalized to a cellular control, APRT, a housekeeping gene. In order to verify that the immunoprecipitation worked efficiently, all ChIP samples were validated by comparing an area enriched in triMe H3K27, the intergenic region upstream of the hoxa5 locus (denoted as upHoxa5) (11) to an underenriched cellular gene (APRT); there is a 2.8-fold enrichment of the upHoxa5 locus relative to that of APRT (Fig. 1A).

Once the ChIP samples were validated, representative genes from all three HSV-1 gene classes were examined. Specifically, these genes were ICP0, ICP27, and ICP4 for immediate-early, tk for early, and gC for late gene classes (Fig. 1B). Our results indicate that triMe H3K27 PTMs are significantly enriched across the HSV-1 genome (Fig. 1B). Interestingly, the degree of enrichment varied among the HSV-1 genes examined, with no clear correlations between gene classes and accumulation of facultative marks. Immediate-early genes ICP0 and ICP27 had similar relative quantities of triMe H3K27, while ICP4 had significantly less (a P value of <0.05 relative to ICP0; ANOVA), suggesting that ICP4 might not be regulated by facultative heterochromatin to the same extent. This also demonstrates that heterochromatin deposition is not dependent on the gene class but is unique to each gene. Furthermore, the early gene tk and late gene gC have relative quantities of triMe H3K27 similar to those of ICP0 and ICP27. To verify that the triMe H3K27 antibody was acting in a specific manner, a control was performed using rabbit anti-mouse IgG antibody; the

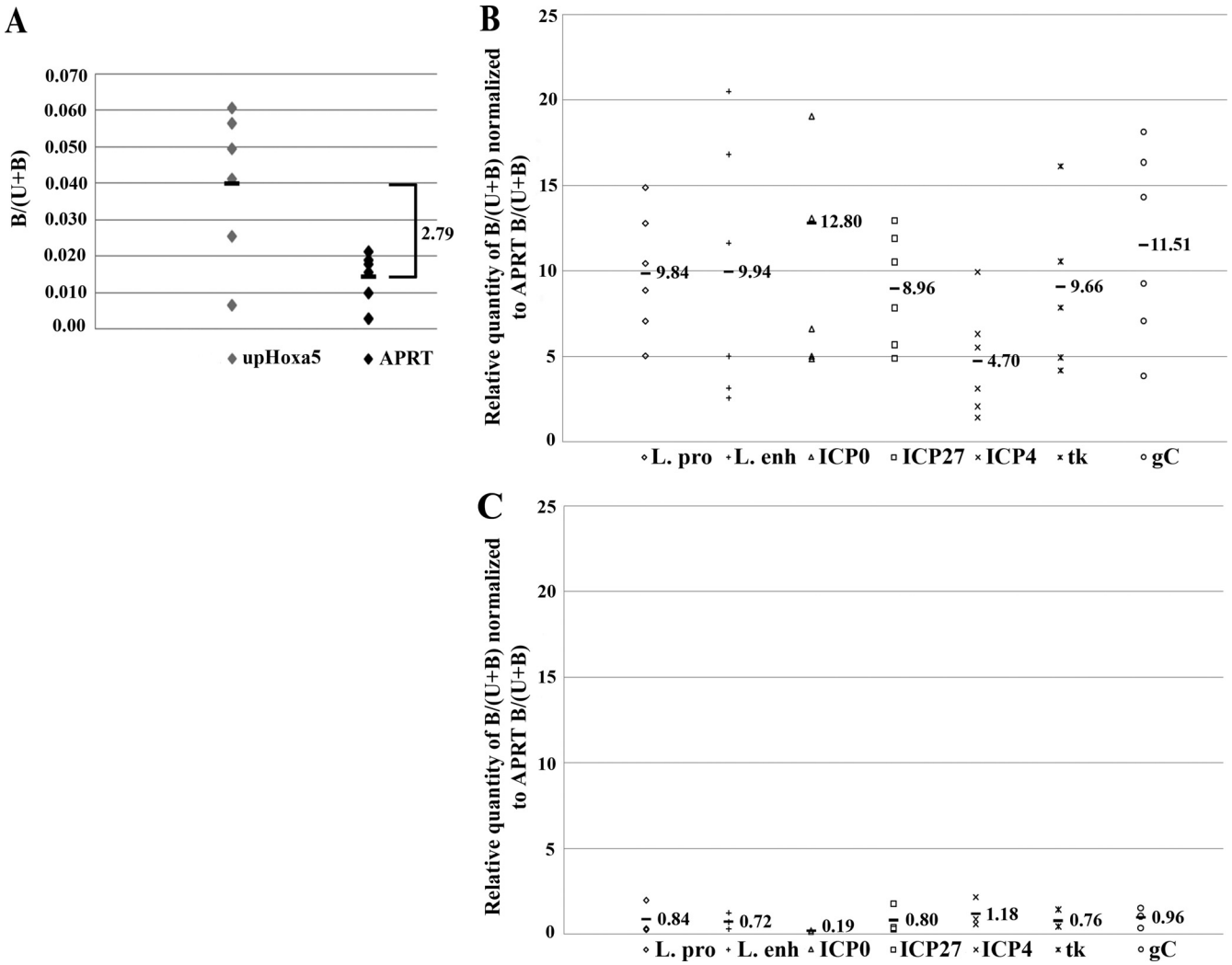

FIG. 1. triMe H3K27 is enriched on the 17*syn*+ latent genome. (A) Validation of the ChIPs using anti-triMe H3K27 was performed by analyzing bound and unbound fractions of ChIP by real-time PCR with positive control PCR primers/probe to upHoxa5 compared to a negative control PCR primer/probe, APRT. Data are graphed as the B/(U+B) ratio. Average fold enrichment between upHoxa5 and APRT is denoted by the bracket. (B) ChIPs using anti-triMe H3K27 were subjected to real-time PCR using primers specific for the HSV-1 target genes indicated, and the results were graphed as B/(U+B) ratio normalized to the APRT B/(U+B). Mean values are displayed for each gene; data from six independent ChIPs are graphed ($n = 6$). (C) ChIPs of latently infected mouse DRG using control IgG were performed and analyzed as described for panel B. Mean values for each gene are shown ($n = 3$). L. pro, LAT promoter; L. enh, LAT enhancer.

results of this precipitation confirmed that the triMe H3K27 precipitations were specific (Fig. 1C). In summary, these data indicate that triMe H3K27 accumulation on the latent genome is not limited to one gene class or region of the genome but is widespread.

macroH2A is incorporated into HSV chromatin on lytic genes during latency. Because triMe H3K27 was found to be associated with the latent HSV-1 genome, we sought to determine whether another characteristic component of facultative heterochromatin was present on the latent genomes. macroH2A is a histone H2A variant enriched in areas of facultative heterochromatin. ChIP assays for macroH2A were successfully validated by comparing a gene on the X chromosome, midline, that is known to be enriched in macroH2A to an underenriched cellular control, upHoxa5 (1) (Fig. 2A). As with the triMe H3K27 ChIP assays, macroH2A was enriched on chromatin associated with all HSV-1 lytic genes and the LAT region (Fig. 2B). Immediate-early gene ICP4 appeared to be the most enriched in this histone variant relative to the other lytic genes but it was not statistically significant, suggesting that there is an equal deposition of macroH2A over the lytic genes. Interestingly, a trend was observed in which the LAT enhancer was more greatly enriched relative to the LAT promoter and several other lytic targets. In summary, our results demonstrate that macroH2A, a measure of facultative heterochromatin, has replaced at least some of the H2A present in the histone octamer in the chromatin on all HSV-1 gene targets. The relative amounts of macroH2A are also independent of gene class and are unique from the pattern of triMe H3K27 enrichment. Overall, the results of the triMe H3K27 and macroH2A ChIP experiments indicate that all regions of the HSV-1 latent genome examined are enriched in

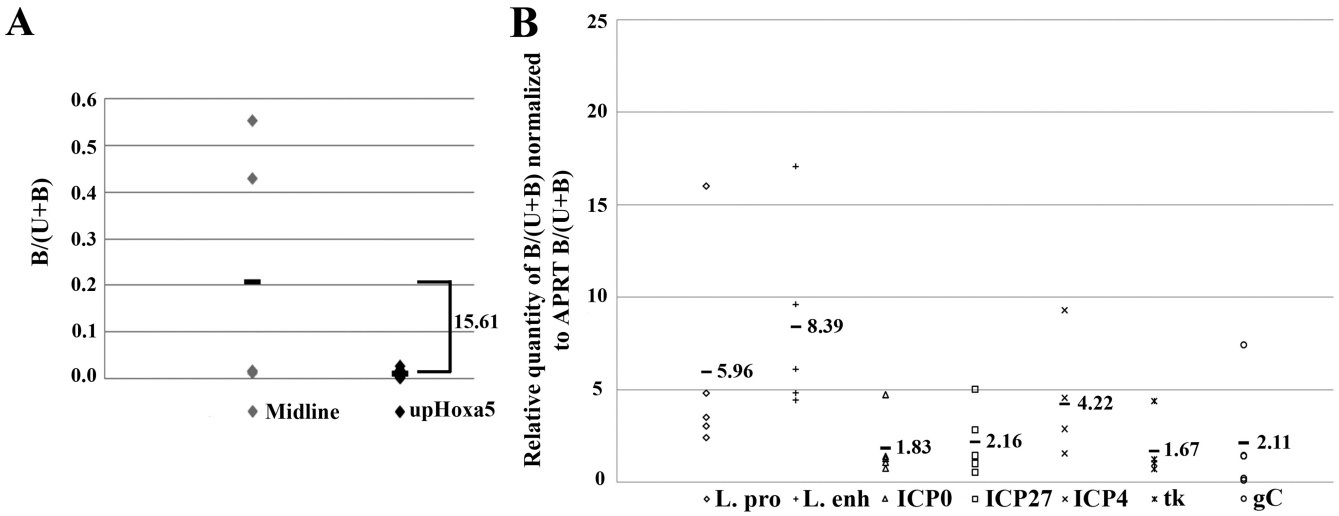

FIG. 2. Histone variant macroH2A is incorporated into the viral chromatin on the 17*syn*+ latent genome. ChIP of histone variant macroH2A on 17*syn*+ latently infected mouse DRG. (A) Validation of the ChIPs with anti-macroH2A were performed by analyzing bound and unbound fractions of ChIP by real-time PCR with positive control PCR primers/probe to midline compared to negative control PCR primers/probe, upHoxa5. Data were graphed as the B/(U+B) ratio. Average fold enrichment between midline and upHoxa5 is denoted by the bracket. (B) ChIPs using anti-macroH2A were subjected to real-time PCR using primers specific for the HSV-1 target genes indicated, and the results were graphed as B/(U+B) normalized to APRT B/(U+B). Mean values for each gene are shown; data from six independent ChIPs are graphed ($n = 6$). L. pro, LAT promoter; L. enh, LAT enhancer.

these marks, and this finding suggests that facultative heterochromatin formation may play a role in gene silencing during latency.

HSV-1 latent genome is enriched in the constitutive heterochromatin PTM triMe H3K9. The previous findings suggest that the HSV-1 genome is significantly enriched in facultative heterochromatin. To determine if the latent genome is enriched only in facultative heterochromatin marks, we also investigated a PTM representative of constitutive (irreversible) heterochromatin. ChIPs were performed with antibody to triMe H3K9 and were validated by comparing enrichment levels between a classic constitutively heterochromatic region (mouse centromere) and the housekeeping gene APRT (18). This validation indicated that the mouse centromere was 3.75-fold more enriched in triMe H3K9 than APRT (Fig. 3A). Surprisingly, we found that triMe H3K9 was also enriched on the latent HSV-1 genome (Fig. 3B). Like both facultative heterochromatin marks examined, this PTM was present over most gene targets examined, including the LAT region (promoter and enhancer) and immediate-early and early genes

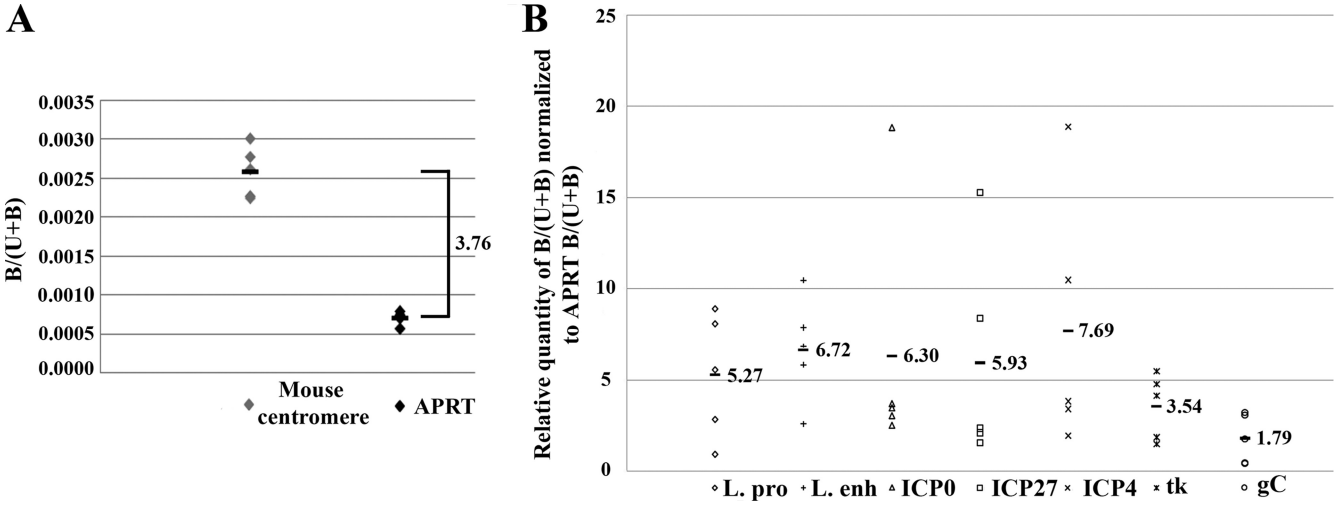

FIG. 3. triMe H3K9 is enriched on the 17*syn*+ latent genome. (A) Validation of the ChIPs using anti-triMe H3K9 were performed by analyzing bound and unbound fractions of ChIP by real-time PCRs with positive control PCR primers/probe to mouse centromere compared to negative control PCR primers/probe, APRT. Data were graphed as the B/(U+B) ratio. Average fold enrichment between mouse centromere and APRT is denoted by the bracket. (B) ChIPs using anti-triMe H3K9 were subjected to real-time PCR using primers specific for the HSV-1 target genes indicated, and the results were graphed as B/(U+B) normalized to APRT B/(U+B). Mean values for each gene are shown; data from five independent ChIPs are graphed ($n = 5$). L. pro, LAT promoter; L. enh, LAT enhancer.

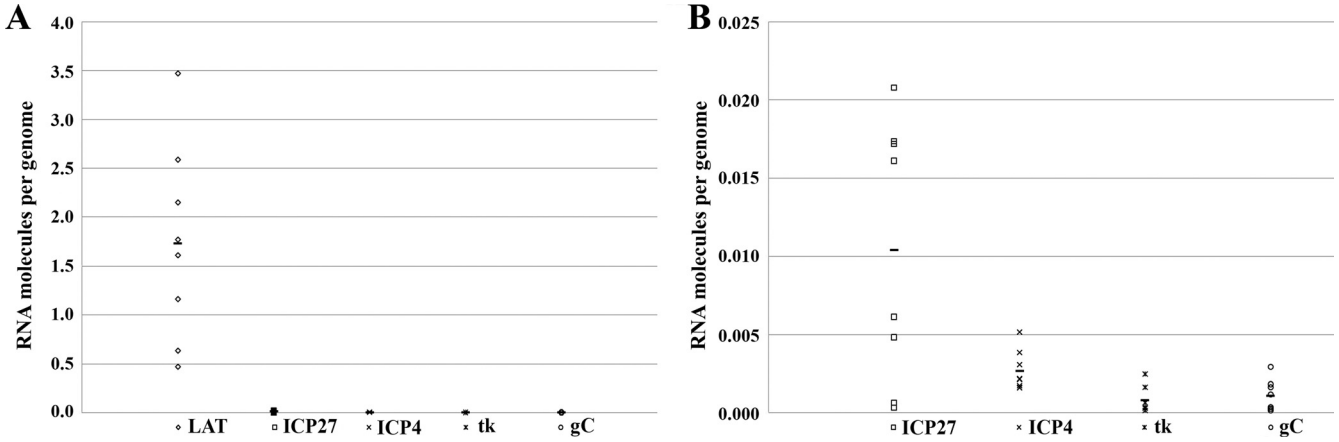

FIG. 4. Viral transcript abundance in 17*syn*+ latently infected mouse DRG. RNA was isolated from latently infected DRG, reverse transcribed into cDNA, and analyzed by real-time PCR as described in Materials and Methods. Data are shown as RNA molecules per genome. (A) Results of PCR analysis for the LAT (5′ exon) and lytic genes. (B) Results of PCR analysis for the lytic genes (note different scale).

(Fig. 3B). Though the late gene gC did not seem to correlate with the other genes in accumulation of triMe H3K9, it was not significantly different from other viral targets examined. In summary, these data suggest that the HSV-1 genome is significantly enriched in both constitutive and facultative heterochromatin marks during latency. The implications of this are considered in Discussion.

Transcript levels of the LAT and ICP4 during latency do not correlate with heterochromatin enrichment. Since some lytic genes that were examined had higher levels of enrichment in heterochromatic marks than others (ICP4), we sought to determine if genes with more heterochromatin were more transcriptionally repressed. Total RNA and DNA were isolated from latently infected mouse DRG using guanidine thiocyanate extraction. The samples were processed into cDNA by reverse transcription, and quantitative real-time TaqMan PCR was performed. RNA molecules per genome were calculated for the LAT, ICP27, ICP4, tk, and gC genes, as shown in Fig. 4. As expected, the LAT primary transcript was the most abundant RNA detected, with a mean of 1.5 molecules per genome (Fig. 4A). To visualize the differences between the lytic genes examined, we removed the LAT data set and regraphed the lytic genes separately on a different scale (Fig. 4B). This manner of graphing the data revealed that ICP27 had significantly higher levels of transcripts than ICP4, tk, and gC ($P < 0.05$). Furthermore, ICP4 had more molecules per genome than tk and gC, which showed similar levels of transcript accumulation ($P < 0.05$). This suggests that not all lytic transcripts are expressed or repressed during latency to the same degree, in agreement with previous studies (2, 8, 12). When the transcription data are compared to the heterochromatin enrichment levels described earlier, some of the investigated genes show a correlation between transcript levels and heterochromatin enrichment, in which higher enrichment of heterochromatin corresponds to lower transcript abundance. Specifically, ICP4 had the lowest level of enrichment of triMe H3K27 (Fig. 1B) relative to other genes and a higher transcript abundance during latency relative to tk and gC, suggesting a relationship between faultative heterochromatin deposition and transcript abundance. ICP27, however, did not show a clear correlation between transcript abundance and triMe H3K27 enrichment as it had relatively greater amounts of heterochromatin than ICP4 but also a fourfold enrichment in transcript abundance. A similar pattern was observed for the LAT enhancer. In summary, this indicates that the transcription status of only some genes is reflective of its facultative heterochromatin status. Other mechanisms may be in place for the transcriptional repression of ICP4 and the enriched heterochromatin deposition on the LAT.

The LAT regulates enrichment of facultative heterochromatin marks. Since LAT mutants display leakier lytic transcript abundance in the mouse, we investigated whether this is due to an altered repression through facultative heterochromatin deposition. Therefore, we performed ChIP on a LAT promoter mutant, 17ΔPst, assaying for the presence of triMe H3K27 and macroH2A. In the absence of the LAT, a dramatically different pattern of enrichment is seen on the latent genome than was observed for 17*syn*+. An increase in enrichment of the facultative heterochromatin mark triMe H3K27 was observed on latent 17ΔPst genomes (Fig. 5) (Table 1). While lytic genes gC and tk showed roughly the same amount of triMe H3K27 enrichment as was observed for 17*syn*+, the LAT enhancer, ICP0, ICP27, and ICP4 all showed increases in enrichment (3.0-, 2.0-, 1.7-, and 5.0-fold, respectively). However, only the increases noted on the LAT enhancer, ICP0, and ICP4 were significantly different between 17*syn*+ and 17ΔPst (Table 1).

Similarly, in the case of macroH2A on 17ΔPst, all genes examined showed increased enrichment compared to *17syn*+ (Fig. 6) (Table 2). The most dramatic increases seen were enrichment on ICP0 (sixfold), ICP27 (3.5-fold), and tk (threefold); however, only lytic gene ICP0 displayed a significantly different enrichment (Table 2). Taken together, these differences in incorporation suggest that the LAT plays some role in regulating the amount of both triMe H3K27 and macroH2A that is incorporated into the viral chromatin in a gene-specific manner.

PRC1 protein Bmi1 associates with the latent genome. It was found that triMe H3K27 is present on the genome during latency. The only mammalian histone methyltransferase

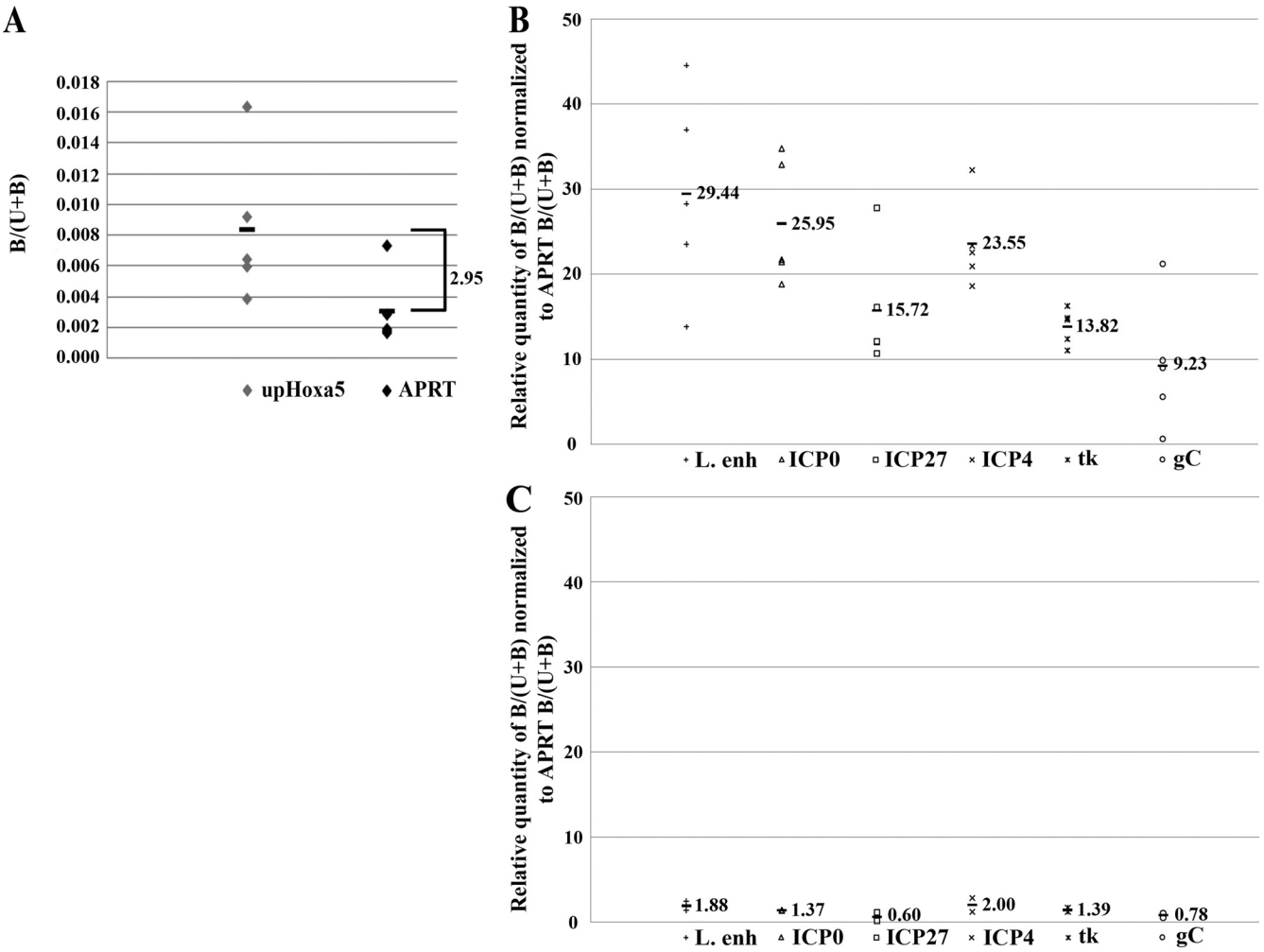

FIG. 5. triMe H3K27 enrichment is increased on the 17ΔPst latent genome. (A) Validation of the ChIPs using anti-triMe H3K27 was performed by analyzing bound and unbound fractions of ChIP by real-time PCR with positive control PCR primers/probe to upHoxa5 compared to negative control PCR primers/probe, APRT. Data were analyzed as the B/(U+B) ratio. Average fold enrichment between upHoxa5 and APRT is denoted by the bracket. (B) ChIPs using anti-triMe H3K27 were subjected to real-time PCR using primers specific for the HSV-1 target genes indicated, and the results were graphed as B/(U+B) normalized to APRT B/(U+B). Mean values for each gene are shown; data from five independent ChIPs are graphed ($n = 5$). (C) ChIPs of latently infected mouse DRG using control IgG were performed and analyzed as described for panel B. Mean values for each gene are shown ($n = 2$). L. enh, LAT enhancer.

TABLE 1. Mean normalized values of triMe H3K27 enrichment for 17*syn*+ and 17ΔPst

Primer target	B/(U+B) value		Fold difference[c] 17ΔPst/17*syn*+	*P* value[d]
	17*syn*+[a]	17ΔPst[b]		
LAT promoter	9.84	NA		
LAT enhancer	9.94	29.44	2.96	<0.0001
ICP0	12.80	25.95	2.03	<0.0001
ICP27	8.96	15.72	1.75	0.35
ICP4	4.70	23.55	5.00	<0.0001
tk	9.66	13.82	1.43	0.95
gC	11.51	9.23	0.80	1.00

[a] Mean values of B/(U+B) normalized to APRT B/(U+B) are listed from ChIPs using anti-triMe H3K27 in 17*syn*+ latently infected mouse DRG (Fig. 1).
[b] Mean values of B/(U+B) normalized to APRT B/(U+B) are listed from ChIPs using anti-triMe H3K27 in 17ΔPst latently infected mouse DRG (Fig. 5). NA, not applicable.
[c] Fold enrichment of 17ΔPst B/(U+B) values relative to 17*syn*+ B/(U+B) values.
[d] *P* values between the values in columns 2 and 3 were determined by ANOVA (see Materials and Methods).

(HMT) known to catalyze triMe H3K27 in vivo is EZH2, a member of the Polycomb repressive complex 2 (PRC2) (20a). PRC2 is a multiprotein complex that assists in Polycomb group protein silencing along with another multiprotein complex, PRC1. PRC2, also known as the "establishment complex," acts to initially repress a gene by establishing triMe H3K27. PRC2 is later replaced by PRC1, which acts to maintain the repressive marks on the gene and is referred to as the "maintenance complex." Since triMe H3K27 was enriched on the HSV-1 latent genome, this indicated that the Polycomb group proteins might be binding on the genome. Therefore, we decided to investigate if one set of these cellular proteins was interacting with the latent HSV-1 genome. Since we demonstrated that the triMe H3K27 marks are already established at latency, we hypothesized that the maintenance PRC1 complex would be the most likely PRC bound to the HSV-1 genome at this time. To determine if repression of HSV-1 lytic genes during latency

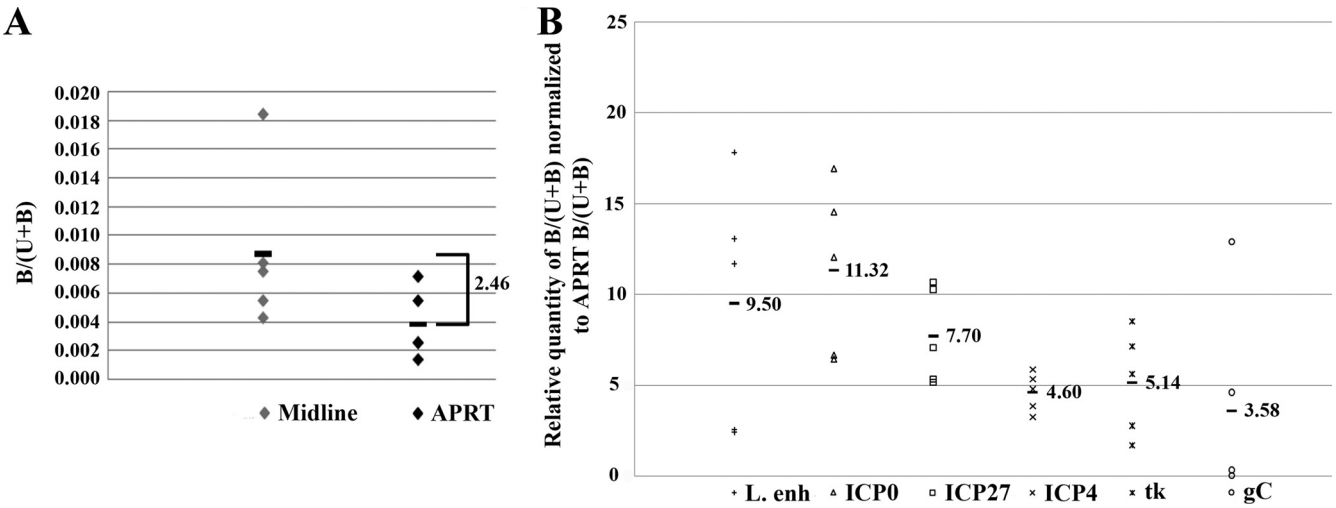

FIG. 6. macroH2A replacement in the viral chromatin is increased on the 17ΔPst latent genome. (A) Validation of the macroH2A ChIPs was performed by analyzing bound and unbound fractions of ChIPs by real-time PCR with positive control PCR primers/probe to midline compared to negative control PCR primers/probe, APRT. Data were analyzed as the B/(U+B) ratio. Average fold enrichment between midline and APRT is denoted by the bracket. (B) ChIPs using anti-macroH2A were subjected to real-time PCR using primers specific for the HSV-1 target genes indicated, and the results were graphed as B/(U+B) normalized to APRT B/(U+B). Mean values for each gene are shown; data from five independent ChIPs are graphed ($n = 5$). L. enh, LAT enhancer.

might be regulated by Polycomb-mediated repression, we performed ChIP assays with an antibody to Bmi1, a member of the PRC1 maintenance complex, to look for association of this protein with the latent genome. Validation of this ChIP was performed by comparing a cellular gene known to bind PRC (HOTAIR) to a cellular gene that does not bind this protein (myo1D) (1) (Fig. 7A). Comparison to negative controls included ChIP using mouse IgG serum (Fig. 1C) as well as an internal viral control, the intron of ICP0 (Fig. 7). Analysis of the latent HSV-1 genome showed enrichment for all regions examined except for the intron of ICP0 (Fig. 7B), while other viral targets had a relatively greater enrichment of this protein, including the LAT enhancer ($P < 0.05$). The LAT enhancer was also more greatly enriched than the LAT promoter and ICP27 ($P < 0.05$). This indicates that while Bmi1 binds to the latent viral genome, it may be binding to specific regions, such as the LAT enhancer. In summary, these data indicate that the PRC1 maintenance complex binds to the HSV-1 genome during latency, consistent with the presence of the triMe H3K27 facultative heterochromatin mark.

TABLE 2. Mean normalized values of macroH2A enrichment for 17*syn*+ and 17ΔPst

Primer target	B/(U+B) value		Fold difference in 17ΔPst/17*syn*+[c]	*P* value[d]
	17*syn*+[a]	17ΔPst[b]		
LAT promoter	5.96	NA		
LAT enhancer	8.39	9.50	1.13	1.00
ICP0	1.83	11.32	6.19	0.016
ICP27	2.16	7.70	3.57	0.85
ICP4	4.22	4.60	1.09	1.00
tk	1.67	5.14	3.08	0.99
gC	2.11	3.58	1.70	1.00

[a] Mean values of B/(U+B) normalized to APRT B/(U+B) are listed from ChIPs using anti-macroH2A in 17*syn*+ latently infected mouse DRG (Fig. 1).
[b] Mean values of B/(U+B) normalized to APRT B/(U+B) are listed from ChIPs using anti-macroH2A in 17ΔPst latently infected mouse DRG (Fig. 5). NA, not applicable.
[c] Fold enrichment of 17ΔPst B/(U+B) values relative to 17*syn*+ B/(U+B) values.
[d] *P* values between the values in columns 2 and 3 were determined by ANOVA (see Materials and Methods).

DISCUSSION

The mechanism behind repression of the HSV-1 lytic genes during latency is presently unclear. We sought to shed light on this issue by investigating the epigenetic histone marks associated with the lytic genes. We hypothesized that the lytic genes would be enriched in facultative heterochromatin due to its reversible nature. By performing ChIP, we found that the genome was enriched not only in facultative marks (triMe H3K27 and macroH2A) but also in constitutive PTMs (triMe H3K9). The presence of heterochromatin confirms that cellular enzymes interact with the viral genome to confer repression during latency. Since both kinds of heterochromatin are present on the genome, it indicates interaction with two different kinds of HMTs. Usually the HMT EZH2 (triMe H3K27) of the PRC and SUV39H (triMe H3K9) catalyze methyl marks in facultative and constitutive heterochromatin, respectively. Our data therefore indicate that there must be two independent mechanisms acting to repress HSV-1 genomes, one that promotes facultative heterochromatin and one that promotes constitutive heterochromatin. It is not clear, however, how these marks on the viral genome are divided. It is possible that these marks are present on different genomes within the same latently infected cell or that all of the marks on the genomes within a given cell are the same, resulting in cells with facultative marks and cells with constitutive marks.

We also noted that the LAT enhancer, previously characterized as euchromatic, also had enrichment of heterochromatic marks. While this could indicate that both types of chromatin marks are on the same region of DNA, it seems more likely that the presence of heterochromatin marks is a result of

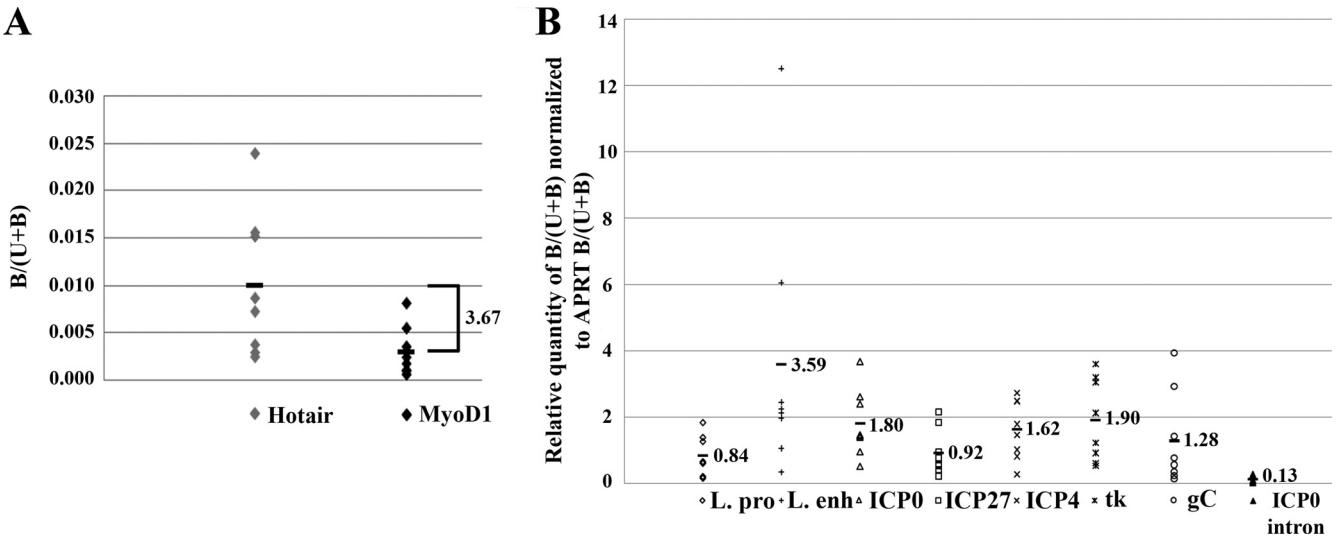

FIG. 7. Bmi1 is enriched on the 17*syn*+ latent genome. (A) Validation of the ChIPs using anti-Bmi1 was performed by analyzing bound and unbound fractions of ChIPs by real-time PCR with positive control PCR primers/probe to HOTAIR compared to negative control PCR primers/probe, myoD1. Data were graphed as the B/(U+B) ratio. Average fold enrichment between HOTAIR and myoD1 is denoted by the bracket. (B) ChIPs using anti-Bmi1 were subjected to real-time PCR using primers specific for the HSV-1 target genes indicated, and the results were graphed as B/(U+B) normalized to APRT B/(U+B). Mean values for each gene are shown; data from eight independent ChIPs are graphed ($n = 8$). L. pro, LAT promoter; L. enh, LAT enhancer.

a lack of LAT transcription. It has been estimated that only one-third of latent genomes express the LAT (9, 16), meaning that two-thirds of the genomes do not express the LAT. The difference in transcription patterns between these two populations of genomes (LAT positive and LAT negative) may explain the difference in chromatin deposition. Genomes expressing LAT would be associated with euchromatic marks, while those not expressing LAT would be associated with heterochromatin. These data support previous papers indicating that there are two populations of latent genomes within sensory ganglia that show differing LAT expression.

The presence of both types of heterochromatin on the LAT enhancer region raises several questions. One hypothesis to explain this observation is that the non-LAT-expressing genomes can be further divided into two subcategories, those associated with constitutive PTMs and those associated with facultative PTMs. The genomes associated with the latter may be more prone to reactivation, even without transcription of the LAT, due to the reversible nature of this type of chromatin. Alternatively, both marks may be present on the same histone protein. In *Arabidopsis* species, both methyl H3K9 and H3K27 can be found on the same H3 protein and are required for binding of certain proteins such as the DNA methyltransferase *CHROMOMETHYLASE3* (15). Further experiments would need to be completed at the single-cell level to help shed light on this issue. Even then, it might be difficult to interpret the results if genomes within the same cell harbor differing PTMs. It is also possible that in terms of the LAT enhancer, one copy of the LAT gene within the genome may be associated with one PTM, while the other copy is associated with a different type. Another less likely explanation for the presence of both marks is that triMe H3K9 incorporation into the genome assumes a different function than in mammalian cells. Constitutive heterochromatin in plants is marked by methyl and diMe H3K9, not triMe H3K9 (7). The virus may have adapted its own definition of histone PTMs in the viral chromatin, meaning that triMe H3K9 may be representative of something other than constitutive heterochromatin (i.e., euchromatin). However, this seems unlikely because the host cell is mammalian and the relative quantities between the LAT enhancer and all the lytic genes examined are similar.

To determine if the LAT, the abundant noncoding RNA expressed during latency, affected enrichment in heterochromatic marks, we performed ChIP assays on the LAT mutant virus, 17ΔPst. Giordani et al. previously showed that there was no difference in accumulation of triMe H3K9 between 17*syn*+ and 17ΔPst (8). In 17ΔPst, we noted a difference in the accumulation of triMe H3K27 and macroH2A incorporation. We found a significant increase in enrichment of both facultative marks in the LAT deletion mutant 17ΔPst. The increased amount of facultative heterochromatin in the absence of LAT suggests that the lytic genes are in a state more ready to revert back to euchromatin than they are in 17*syn*+. This correlates with transcription studies in which LAT was shown to have a repressive function, and in the absence of LAT, a leakier transcription profile during latency was observed (2).

While it is clear that the LAT has an effect on the formation of chromatin on the genome, it is not clear if it is the LAT RNA itself, the act of transcribing the LAT, or the DNA-binding sequences removed in 17ΔPst that are important for interaction with these cellular proteins. A balance of facultative heterochromatin markers is maintained by interaction with Polycomb proteins and trithorax proteins (10). It seems possible that deletion of the 202-bp segment of the LAT promoter may have ablated binding of a component of the trithorax protein complex, therefore causing misregulation of the facultative heterochromatin formation on the latent HSV-1 genome.

Based on the evidence of triMe H3K27 enrichment of the HSV-1 genome, we investigated if Polycomb group proteins were involved in the maintenance of these marks during la-

tency. To demonstrate that the PRC1 complex interacts with the HSV-1 genome during latency, we performed ChIP on latently infected mouse DRG using an antibody to a component of the PRC1 complex, Bmi1. Our data indicated that distinct regions of the genome exhibit enrichment of this Polycomb protein. These experiments suggest that PRC1 binds to the genome and maintains the repressive triMe H3K27 marks present on the genome. Overall, this displays a new mechanism for the establishment and maintenance of latency through the use of the cellular Polycomb group proteins.

Repression of lytic genes on the HSV-1 latent genome seems to be of a complex nature that is partly controlled though epigenetic regulation. It is possible that heterochromatin formation on the latent episome is a default host defense mechanism to silence exogenous DNA and that the virus has evolved a mechanism to alter this process and promote preferential deposition of heterochromatic marks that favor reversible silencing of the lytic genes. Control of the facultative heterochromatin may be due in part to LAT-binding components of the trithorax protein group to regulate chromatin deposition. By introducing a certain heterochromatic marker onto the genome, such as triMe H3K27, the virus partakes in the cellular mechanism of repression and maintenance of the repressive marks on the genome by interacting with Polycomb complexes. The virus is then able to use the PRC1 complex to maintain the repressive marks on the genome, which would be advantageous in controlling reactivation from latency. However, the genes are not locked into a repressive state, since the PRC1 proteins can be removed, allowing transcription factors to access the DNA. To our knowledge, this is the first example of a virus interacting with cellular proteins of the Polycomb group to repress transcription on its genome.

ACKNOWLEDGMENTS

This work was supported in part by NIH grant R01 AI48633 and an Investigator in the Pathogenesis of Infectious Disease Award from the Burroughs Wellcome Fund to D.C.B. D.L.K. was supported by training grants T32 AI007110 and T32 AI060527 from the NIH.

We also acknowledge helpful comments on the manuscript from N. Giordani, C. Lilly, and L. Watson.

ADDENDUM IN PROOF

At the proof stage of this article, the authors became aware of a report by Cliffe et al. (A. R. Cliffe, D. A. Garber, and D. M. Knipe, J. Virol. **83:**8182–8190, 2009) that corroborates our data. In their study, triMe H3K27 was enriched on latent HSV-1 genomes, and the degree of enrichment was directly related to LAT expression. A key difference between our findings, however, was that the LAT promoter mutant in their study is less enriched in triMe H3K27 than wild-type HSV-1, whereas our LAT promoter mutant exhibits significantly more enrichment than the wild type. It is our belief that this difference is most likely due to the HSV-1 strain; our study used 17syn+, whereas the Cliffe et al. study used KOS. These two strains have significant biological differences in both the acute and the latent phases of their infection. In addition to the strain difference, the site of latency that was investigated might also be a factor as we utilized the DRG, whereas Cliffe et al. examined the TG. Clearly, it will require additional experiments to determine if one of these factors is responsible for the difference in LAT-dependent H3K27 triMe observed.

REFERENCES

1. **Changolkar, L. N., and J. R. Pehrson.** 2006. macroH2A1 histone variants are depleted on active genes but concentrated on the inactive X chromosome. Mol. Cell. Biol. **26:**4410–4420.
2. **Chen, S. H., M. F. Kramer, P. A. Schaffer, and D. M. Coen.** 1997. A viral function represses accumulation of transcripts from productive-cycle genes in mouse ganglia latently infected with herpes simplex virus. J. Virol. **71:** 5878–5884.
3. **Chirgwin, J. M., A. E. Przybyla, R. J. MacDonald, and W. J. Rutter.** 1979. Isolation of biologically active ribonucleic acid from sources enriched in ribonuclease. Biochemistry **18:**5294–5299.
4. **Devi-Rao, G. B., D. C. Bloom, J. G. Stevens, and E. K. Wagner.** 1994. Herpes simplex virus type 1 DNA replication and gene expression during explant-induced reactivation of latently infected murine sensory ganglia. J. Virol. **68:**1271–1282.
5. **Doyen, C. M., W. An, D. Angelov, V. Bondarenko, F. Mietton, V. M. Studitsky, A. Hamiche, R. G. Roeder, P. Bouvet, and S. Dimitrov.** 2006. Mechanism of polymerase II transcription repression by the histone variant macroH2A. Mol. Cell. Biol. **26:**1156–1164.
6. **Edwards, D., and J. J. Berry.** 1987. The efficiency of simulation-based multiple comparisons. Biometrics **43:**913–928.
7. **Fischer, A., I. Hofmann, K. Naumann, and G. Reuter.** 2006. Heterochromatin proteins and the control of heterochromatic gene silencing in *Arabidopsis*. J. Plant Physiol. **163:**358–368.
8. **Giordani, N. V., D. M. Neumann, D. L. Kwiatkowski, P. S. Bhattacharjee, P. K. McAnany, J. M. Hill, and D. C. Bloom.** 2008. During HSV-1 infection of rabbits, the ability to express the LAT increases latent-phase transcription of lytic genes. J. Virol. **82:**6056–6060.
9. **Gressens, P., and J. R. Martin.** 1994. In situ polymerase chain reaction: localization of HSV-2 DNA sequences in infections of the nervous system. J. Virol. Methods **46:**61–83.
10. **Grimaud, C., N. Negre, and G. Cavalli.** 2006. From genetics to epigenetics: the tale of Polycomb group and trithorax group genes. Chromosome Res. **14:**363–375.
11. **Kim, S. Y., S. W. Paylor, T. Magnuson, and A. Schumacher.** 2006. Juxtaposed Polycomb complexes co-regulate vertebral identity. Development **133:** 4957–4968.
12. **Kramer, M. F., and D. M. Coen.** 1995. Quantification of transcripts from the ICP4 and thymidine kinase genes in mouse ganglia latently infected with herpes simplex virus. J. Virol. **69:**1389–1399.
13. **Kubat, N. J., A. L. Amelio, N. V. Giordani, and D. C. Bloom.** 2004. The herpes simplex virus type 1 latency-associated transcript (LAT) enhancer/*rcr* is hyperacetylated during latency independently of LAT transcription. J. Virol. **78:**12508–12518.
14. **Kubat, N. J., R. K. Tran, P. McAnany, and D. C. Bloom.** 2004. Specific histone tail modification and not DNA methylation is a determinant of herpes simplex virus type 1 latent gene expression. J. Virol. **78:**1139–1149.
15. **Lindroth, A. M., D. Shultis, Z. Jasencakova, J. Fuchs, L. Johnson, D. Schubert, D. Patnaik, S. Pradhan, J. Goodrich, I. Schubert, T. Jenuwein, S. Khorasanizadeh, and S. E. Jacobsen.** 2004. Dual histone H3 methylation marks at lysines 9 and 27 required for interaction with *CHROMOMETHYL ASE3*. EMBO J. **23:**4286–4296.
16. **Mehta, A., J. Maggioncalda, O. Bagasra, S. Thikkavarapu, P. Saikumari, T. Valyi-Nagy, N. W. Fraser, and T. M. Block.** 1995. In situ DNA PCR and RNA hybridization of herpes simplex virus sequences in trigeminal ganglia of latently infected mice. Virology **206:**633–640.
17. **Milliken, G. A., and D. E. Johnson.** 1984. Analysis of messy data. Lifetime Learning Publications, Belmont, CA.
18. **Nakayama, J., J. C. Rice, B. D. Strahl, C. D. Allis, and S. I. Grewal.** 2001. Role of histone H3 lysine 9 methylation in epigenetic control of heterochromatin assembly. Science **292:**110–113.
19. **Rock, D. L., and N. W. Fraser.** 1985. Latent herpes simplex virus type 1 DNA contains two copies of the virion DNA joint region. J. Virol. **55:**849–852.
20. **Rock, D. L., A. B. Nesburn, H. Ghaisi, J. Ong, T. L. Lewis, J. R. Lokensgard, and S. L. Wechsler.** 1987. Detection of latency-related viral RNAs in trigeminal ganglia of rabbits latently infected with herpes simplex virus. J. Virol. **61:**3820–3826.

20a. **Schwartz, Y. B., and V. Pirrotta.** 2008. Polycomb complexes and epigenetic states. Curr. Opin. Cell Biol. **20:**266–273.

21. **Stevens, J. G., E. K. Wagner, R. G. B. Devi, M. L. Cook, and L. T. Feldman.** 1987. RNA complementary to a herpesvirus alpha gene mRNA is prominent in latently infected neurons. Science **235:**1056–1059.
22. **Trojer, P., and D. Reinberg.** 2007. Facultative heterochromatin: is there a distinctive molecular signature? Mol. Cell **28:**1–13.
23. **Vakoc, C. R., M. M. Sachdeva, H. Wang, and G. A. Blobel.** 2006. Profile of histone lysine methylation across transcribed mammalian chromatin. Mol. Cell. Biol. **26:**9185–9195.
24. **Wang, Q. Y., C. Zhou, K. E. Johnson, R. C. Colgrove, D. M. Coen, and D. M. Knipe.** 2005. Herpesviral latency-associated transcript gene promotes assembly of heterochromatin on viral lytic-gene promoters in latent infection. Proc. Natl. Acad. Sci. USA **102:**16055–16059.